# On the duration of the embedded phase of star formation

## Kim et al. 2020, arXiv: 2012.00019, submitted to MNRAS

2020/12/16 K.Kushibiki

Feedback from massive stars plays a key role in molecular cloud evolution. After the onset of star formation, the young stellar population is exposed by photoionization, winds, supernovae, and radiation pressure from massive stars. Recent observations of nearby galaxies have provided the evolutionary timeline between molecular clouds and exposed young stars, but the duration of the embedded phase of massive star formation is still ill-constrained. We measure how long massive stellar populations remain embedded within their natal cloud, by applying a statistical method to six nearby galaxies at 20−100 pc resolution, using CO, *Spitzer* 24 $\mu$m, and H$\alpha$ emission as tracers of molecular clouds, embedded star formation, and exposed star formation, respectively. We find that the embedded phase (with CO and 24 $\mu$m emission) lasts for 2–7 Myr and constitutes 17–47% of the cloud lifetime. During approximately the first half of this phase, the region is invisible in H$\alpha$, making it heavily obscured. For the second half of this phase, the region also emits in H$\alpha$ and is partially exposed. Once the cloud has been dispersed by feedback, 24 $\mu$m emission no longer traces ongoing star formation, but remains detectable for another 2–9 Myr through the emission from ambient CO-dark gas, tracing star formation that recently ended. The short duration of massive star formation suggests that pre-supernova feedback (photoionization and winds) is important in disrupting molecular clouds. The measured timescales do not show significant correlations with environmental properties (e.g. metallicity, molecular gas surface density). Future JWST observations will enable these measurements routinely across the nearby galaxy population.

Table 3

| Galaxy | CO vs Hα | | | | CO vs 24 $\mu$m | | | | |
|---|---|---|---|---|---|---|---|---|---|
| | $t_{CO}$ | $t_{fb,H\alpha}$ | $t_{H\alpha}$ | $\lambda$ | $t_{fb,24\mu m}$ | $t_{24\mu m}$ | $\lambda$ | $v_{fb}$ | $\epsilon_{sf}$ |
| | [Myr] | [Myr] | [Myr] | [pc] | [Myr] | [Myr] | [pc] | [km s$^{-1}$] | [per cent] |
| IC 342 | $20.0^{+2.0}_{-2.3}$ | $2.2^{+0.4}_{-0.5}$ | $6.4^{+0.5}_{-0.6}$ | $120^{+10}_{-10}$ | $5.2^{+1.5}_{-2.0}$ | $7.9^{+1.8}_{-2.2}$ | $190^{+59}_{-62}$ | $14.3^{+4.0}_{-1.8}$ | $1.9^{+1.4}_{-0.8}$ |
| LMC | $11.1^{+1.6}_{-1.7}$ | $1.2^{+0.2}_{-0.2}$ | $5.8^{+0.4}_{-0.4}$ | $71^{+13}_{-8}$ | $5.0^{+1.6}_{-2.0}$ | $13.6^{+3.7}_{-4.8}$ | $73^{+38}_{-26}$ | $10.0^{+2.1}_{-1.7}$ | $6.8^{+4.9}_{-3.0}$ |
| M31 | $14.0^{+2.1}_{-1.9}$ | $1.1^{+0.3}_{-0.2}$ | $5.5^{+0.4}_{-0.3}$ | $181^{+28}_{-19}$ | $2.4^{+1.4}_{-0.8}$ | $4.2^{+1.5}_{-0.7}$ | $128^{+97}_{-23}$ | $29.5^{+6.9}_{-5.3}$ | $0.7^{+0.2}_{-0.2}$ |
| M33 | $14.5^{+1.6}_{-1.5}$ | $3.3^{+0.6}_{-0.5}$ | $7.9^{+0.7}_{-0.6}$ | $155^{+30}_{-24}$ | $6.8^{+2.1}_{-2.0}$ | $11.9^{+2.9}_{-2.1}$ | $119^{+60}_{-35}$ | $10.3^{+1.5}_{-1.3}$ | $3.5^{+2.5}_{-1.5}$ |
| M51 | $30.7^{+8.7}_{-4.9}$ | $4.7^{+2.0}_{-1.1}$ | $8.9^{+2.0}_{-1.2}$ | $140^{+25}_{-17}$ | $< 4.0^{a}$ | $3.6^{+1.2}_{-0.9}$ | $< 136^{a}$ | $7.9^{+2.0}_{-2.1}$ | $3.3^{+2.9}_{-1.4}$ |
| NGC 300 | $10.8^{+2.2}_{-1.6}$ | $1.5^{+0.2}_{-0.2}$ | $6.1^{+0.2}_{-0.2}$ | $104^{+22}_{-18}$ | $4.9^{+1.2}_{-1.9}$ | $7.9^{+1.5}_{-2.1}$ | $178^{+125}_{-75}$ | $9.4^{+0.8}_{-0.7}$ | $3.3^{+2.6}_{-1.4}$ |

[a] Only a 1$\sigma$ upper limit can be derived for not satisfying (ii) and (viii) in Section 5.1.

Fig. 2

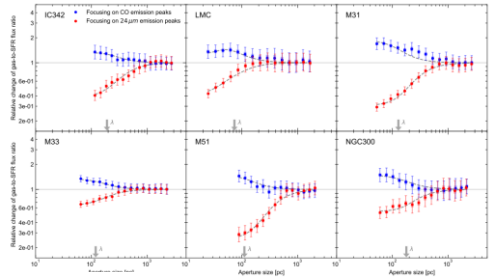


A part of Fig. 3

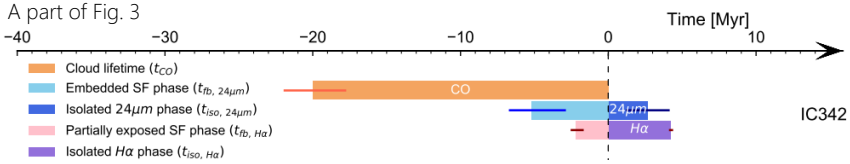


星形成に関わるfeedback(SNe, Stellar)は未だ理解不足
GMCの進化タイムスケールから星形成の物理に迫る

Kruijssen&Longmore 2014 (KL14), Kruijssen+2018

- Small scaleでは星形成則は崩れる
- gas-to-SFR flux ratioの空間スケールによる変化がGMCの進化タイムスケール(~rarity)とその距離間隔に依存するモデル(KL14)
  → Apertureを変えながらgas-to-SFRを測定
  → GMC scaleを分解する必要がない
- CO+Hαが想定されているtracer

Kruijssen+2018 Fig.1

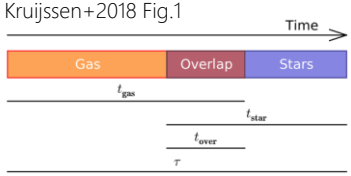


Kruijssen+2018 Fig.2

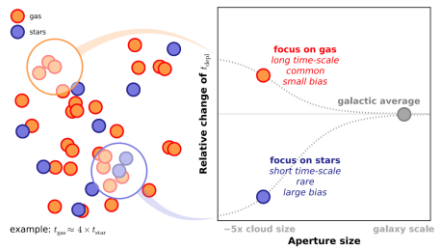


6つの近傍銀河について

- CO : Gas
- *Spitzer*/MIPS24um : Embedded SF
- Hα : Exposed SF

としてGMCの進化タイムスケールに
制限をかけ、feedbackについて示唆を得る

Table 1

| Galaxy | Stellar mass[a] | Metallicity[b,c] | Distance | Inclination | Position angle | CO observations | CO resolution | 24 $\mu$m resolution | Spatial resolution[d] |
|---|---|---|---|---|---|---|---|---|---|
| | [$\log_{10}$ M$_\odot$] | [Z/Z$_\odot$] | [Mpc] | [deg] | [deg] | | [″] | [″] | [pc] |
| IC 342 | 10.2 ± 0.1 | 0.90 ± 0.20 | 3.45 | 31.0 | 42.0 | NOEMA + IRAM 30-m | 3.6 | 6.4 | 107 |
| LMC | 9.3 ± 0.1 | 0.48 ± 0.03 | 0.05 | 22.0 | 168.0 | ATNF | 45 | 6.4 | 11 |
| M31 (NGC 224) | 11.0 ± 0.1 | 0.76 ± 0.20 | 0.78 | 77.7 | 37.7 | CARMA + IRAM 30-m | 5.5 | 6.4 | 24 |
| M33 (NGC 598) | 9.4 ± 0.1 | 0.50 ± 0.06 | 0.84 | 55.0 | 201.1 | IRAM 30-m | 12 | 6.4 | 49 |
| M51 (NGC 5194) | 10.7 ± 0.1 | 1.37 ± 0.20 | 8.6 | 21.0 | 173.0 | PdBI + IRAM 30-m | 1.1 | 2.4 | 100 |
| NGC 300 | 9.3 ± 0.1 | 0.48 ± 0.06 | 2.0 | 42.0 | 111.0 | ALMA | 2.1 | 6.4 | 62 |

- 分子雲は$t_{fb,24um}$=2-7 Myrで拡散 ($t_{CO}$=10-30 Myrの17-47%)
  → 最初の超新星爆発のタイムスケール(4-20 Myr)より短い
  → より初期のfeedback(photoionizationやstellar winds)が重要になる
- 24um放射は分子雲拡散後$t_{24um}$-$t_{fb,24um}$=2-9 Myrで減衰する
- 星形成領域間の距離は~100-200 pc (過去研究とコンシステント)
  → vertical gas disc scale heightと一致 (Kruijssen+2019)
- Star formation efficiency ($\epsilon_{sf}$) = $\Sigma_{SFR}/(\Sigma_{gas}/t_{CO})$ = 0.7-6.8%で非効率な星形成 (過去研究とコンシステント)
- Feedback velocity = $r_{CO}/t_{fb}$ = 10-40 pc (近傍のHII regionの膨張速度とコンシステント)

- MIP24umで探ることができたheavily obscured phase = $t_{obscured}$
  = $t_{fb,24um}$-$t_{fb,H\alpha}$ = 3.0 ± 0.9 Myr
- 他のglobalな物理量との相関は見られなかった
- $t_{24um}$や$t_{iso,24um}$=$t_{24um}$-$t_{fb,24um}$は金属量が増えると減少
  → 金属量が増えるとmassive starsのwindが強くなるためか？
  ($\epsilon_{sf}$に見える相関は金属量が原因か？)

JWST(MIRI: 分解能=0.7″)によって
本手法を適応できる銀河が増える
(MIPS24um : 6.4″)

Fig. 4